J Mater Sci (2011) 46:2726–2732
DOI 10.1007/s10853-010-5145-5

# The effect of contamination on the metallurgy of commercially pure titanium welded with a pulsed laser beam

**Alexander Buddery · Patrick Kelly · John Drennan · Matthew Dargusch**

Received: 16 August 2010 / Accepted: 30 November 2010 / Published online: 16 December 2010


**Abstract** Commercially pure titanium components in medical devices are commonly joined using pulsed laser welding because of the precision, low heat input and low thermal distortion it affords. Despite the importance of this technique in structural components, such as dental prosthesis, there is still a limited understanding of the factors which affect the weld metallurgy. In this study the effect of O, N and Fe on the weld metallurgy, as both external and bulk contaminants, is investigated. The results indicate that Fe has the most pronounced effect on the nature of the allotropic $\beta$–$\alpha$ phase transformation, suppressing the massive transformation and encouraging the formation of martensite. This finding is in contrast to the effects of O and N which are usually the subject of studies reported in the literature. Whilst O and N do cause more hardening than Fe, this seems to be mainly through more pronounced solid solution strengthening. The study also demonstrates the inadequacy of relying on ASTM grades to predict weld properties and the need to adequately characterise the base alloys.

A. Buddery (✉) · P. Kelly · M. Dargusch
School of Mechanical and Mining Engineering,
The University of Queensland, Brisbane, Australia
e-mail: a.buddery@uq.edu.au

J. Drennan
Centre for Microscopy and Microanalysis,
The University of Queensland, Brisbane, Australia

A. Buddery · M. Dargusch
CAST Cooperative Research Centre, Brisbane, Australia

## Introduction

Pulsed laser welding is a commonly used technology to join commercially pure (CP) titanium alloy components in dental prosthesis and other medical devices [1, 2]. Whilst it is known that common contaminants such as O, N and Fe affect the properties of these alloys, questions still remain about their effects on the microstructure and properties of laser welds. These elements not only cause solid solution strengthening, but also affect the nature of the allotropic phase transformation from the high temperature BCC $\beta$ phase to the low temperature HCP $\alpha$ phase that occurs at about 883 °C in pure titanium. A better understanding of the effects of these contaminants might shed light on apparent discrepancies, which exist in the literature with regards to the as-welded microstructure. Whilst many studies report a columnar microstructure in pulsed laser welds of CP titanium [3–5] many others report a predominantly acicular structure [6–8]. As reported by Huang et al. [9] the reasons for this apparent discrepancy remain unclear.

When evaluating the effect of these contaminants on the weld microstructure it is important to consider pre-existing bulk contaminants in the alloy before welding. In the current literature, however, the composition of the bulk material is often not even reported. In some cases the ASTM grade of CP titanium is quoted, but this may not be adequate to characterise the material for the purposes of researching the effect of contaminants. In some cases there may even be no classification given.

The problem is further compounded with the need to consider the uptake of other contaminants during welding. For the case of pulsed laser welding there has been very little evaluation of the effect of these contaminants, largely due to the small size of the weld zone, which makes

analysis difficult. Significant O and N uptake can occur from the atmosphere despite welding under an argon shielding gas. Li et al. [10] studied the effect of adding oxygen contamination to the argon shielding gas during pulsed laser welding of CP titanium and reported that it caused a transition from serrated and acicular α to predominantly acicular α. Unfortunately, however, they did not report the composition of the base alloy they used nor did they directly measure the uptake of contaminants in the weld.

A recent study has also identified that the weld pool can pick up contamination from the underlying stage if it is in close proximity [11]. In that study the authors observed a transition from columnar to acicular α in the fusion zone due to interaction with a gypsum-based stage. They attributed this to a measured increase in O and H contamination, but did not test for other significant contaminants present in the gypsum.

In order to develop a better understanding of the role of key contaminants on weld properties, the effects of O, N and Fe on the morphology and hardness of the microstructure are evaluated in this study. To do this, the effect of bulk contaminants and uptake of external contaminants from the welding atmosphere and a mild steel stage are analysed by direct measurement.

## Materials and methods

### Experimental parameters

Three CP titanium alloys with compositions given in Table 1 were used in the form of 0.5 mm thick sheet for this study. To assess the effects of external contamination, the alloy G1a only was used. Welds of alloy G1a were also compared with the other alloys to assess the effects of bulk contaminants. The process parameters that were varied are given in Table 2. The process parameters kept constant for all trials were a spot diameter of 0.8 mm, 7 ms pulse length, 2 Hz pulse frequency, 60% pulse overlap and square pulse shaping. Under these conditions a pulse power of 1.1 kW is the minimum required for full penetration of the 0.5 mm thick sheet.

**Table 1** Composition of titanium alloys used in this study

| Alloy (Denotation in text) | Composition (ppm) | | | | |
|---|---|---|---|---|---|
| | Ti | O | N | C | Fe |
| Grade 1 (G1a) | bal. | 690 | 47 | 110 | 390 |
| Grade 1 (G1b) | bal. | 220 | <20 | 110 | 1320 |
| Grade 4 (G4) | bal. | 2900 | 71 | 110 | 3280 |

### Equipment setup

The laser device used for this study was a Nd:YAG crystal emitting a 1.06 μm wavelength gaussian distributed beam (DL3000, Dentaurum Group, Germany). Argon shielding gas was delivered to the workpiece at 50 psi (345 kPa) via two 6 mm nozzles for the weld and weld tail. A dual stage regulator (HPT500, BOC Scientific Ltd., Australia) was used to regulate the output pressure from the argon cylinder with a certified helium leak rate of $1 \times 10^{-9}$sccs. The flow rate of argon was adjusted to the desired level using a rotameter with an accuracy of ±1% (N102-05, Aalborg Inc., USA). A linear stage (MX80S, Parker Hannifin Corp., USA) was used to control the motion of the workpiece during welding.

### Microstructure and hardness

Samples for microstructural analysis and hardness testing were made by seam welding 25 × 15 mm coupons together to form coupons 50 × 15 mm. Samples were polished using standard techniques and etched using a solution of 5% HF, 30% $HNO_3$ and 65% $H_2O_2$ by volume. Vickers microhardness measurements were performed across the top centre of each weld seam using a load of 1 kg. The hardness results for each condition are from an average of three weld coupons, with error bars of one standard deviation.

### Analysis of contamination

For analysis of bulk contaminants standard techniques were used. For oxygen and nitrogen contamination which is difficult to measure in titanium inert gas fusion analysis was used as per the ASTM standard technique (E 1409-05). For O and N analysis of the welds 15-mm long laser irradiated seams were overlapped by 50% onto 0.5 mm thick coupons to produce an irradiated area of 10 × 15 mm for gas fusion analysis (ATI Wah Chang, USA). The results show the average of three samples for each condition with error bars of one standard deviation. Fe analysis on welds was performed using the average of 36 points from electron microprobe analysis (Jeol 8200, Japan). Post welding measurements of O and N contamination were made only for the study on alloy G1a. From the study on G1a it was found that the uptake of contamination under good shielding conditions at a pulse power of 1.1 kW was negligible within a small standard deviation (85 ± 38 ppm O and 43 ± 16 ppm N). As these were the only conditions under which alloys G1b and G4 were welded we believe that it is reasonable to assume that no significant contamination took place and the composition of the weld remains predominantly that of the bulk composition in Table 1.

**Table 2** Experimental variable settings used to investigate the various types of contamination

| Types of contamination | Shielding conditions | Stage setup | Pulse power (kW) | Alloys |
|---|---|---|---|---|
| Bulk | 10l/min flow rate, nozzle 3 mm from workpiece | Titanium stage, 3 mm from workpiece | 1.1 | G1a, G1b, G4 |
| Low | | | 1.1, 1.27, 1.43, 1.6 | G1a |
| Stage | | Mild steel stage, 1.5 mm from workpiece | | |
| Air | 5l/min flow rate, nozzle 9 mm from workpiece | As for 'Bulk' and 'Low' conditions | | |

## Results

### Effect of external contaminants

The fusion zone microstructures for the samples with stage contamination, air contamination and low contamination are given in Fig. 1. Under the low contamination conditions there appears to be little change in microstructure with increasing pulse power. All the samples welded under low contamination conditions exhibited columnar α grains in the fusion zone with irregular grain boundaries. These observations agree well with the hardness results, which also show little change in this condition (Fig. 2a). Low levels of N contamination were observed for all pulse powers under conditions of low contamination. However, the level of oxygen contamination was most affected and increased up to about 350 ppm at the highest pulse power (Fig. 2b, c). It is worth clarifying that the levels of contamination given in Fig. 2b–d refer to the uptake of additional O, N and Fe above the bulk concentration.

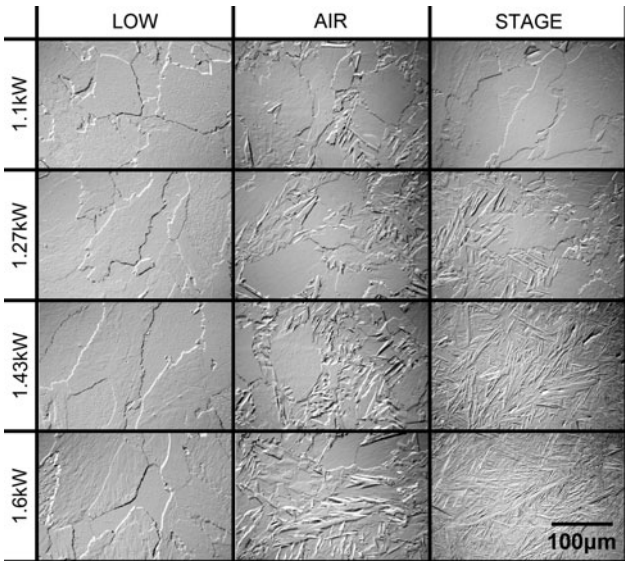


**Fig. 1** Microstructures for low, air and stage contamination conditions at different pulse powers showing: columnar α under conditions of low contamination which does not appear to change with increasing pulse power; columnar α and portions of acicular α which increase with pulse power for conditions of air contamination; and columnar α at low pulse powers which becomes predominantly fine acicular α with increasing pulse power for conditions of stage contamination

Under 'air' contamination conditions there was a significant uptake of both O and N contamination, which appears to increase almost linearly with pulse power (Fig. 2b, c). The O and N contamination appear to have caused significant hardening of the weld seam Fig. 2a. A change is also apparent in the fusion zone microstructure with the formation of increasing portions of acicular α as the level of O and N concentration increases with the pulse power (Fig. 1). However, there still remains a significant portion of columnar α at all pulse powers.

For those samples welded in close proximity to the steel stage at a pulse power of 1.27 kW a significant portion of the microstructure is coarse acicular α and at 1.43 kW the microstructure appears to consist entirely of finer acicular laths (Fig. 1). At the highest pulse power of 1.6 kW these laths become even finer. These observed changes in the fusion zone under conditions of stage contamination are even more dramatic than those observed under 'air' conditions. This is despite there being a lower level of O and N contamination (Fig. 2b, c). There was however an increasing level of Fe contamination with pulse power indicating interaction with the stage (Fig. 2d). Despite the more dramatic changes in microstructure of the samples with Fe contamination from the stage, most of the hardness values for these samples were lower than those with higher O and N contamination, which were welded under 'air' (Fig. 2a).

In addition to changes in the microstructure, evidence of contamination could be seen on the surface of some of the weld seams. For samples welded under low contamination conditions the weld seam was predominantly a shiny silver colour indicating that a thin layer of titanium oxide had formed on the surface after welding. Samples welded at higher pulse powers did begin to show evidence of different coloured oxides at the end of the seam, however, this was minimal. A brown discolouration was observed on the underside of all the samples welded in close proximity to the stage, except for the lowest pulse power of 1.1 kW.

Clear evidence of atmospheric contamination was observed on the weld seam for samples welded under 'air' shielding conditions on both the top and bottom of the

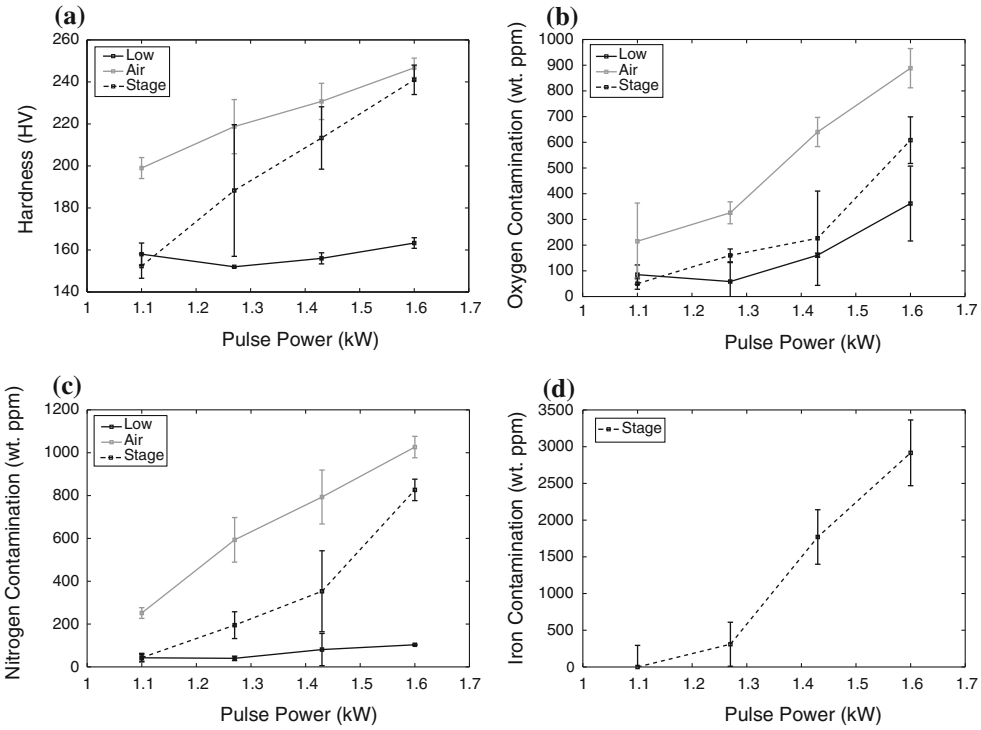


**Fig. 2** Results for **a** fusion zone hardness and additional uptake of **b** oxygen, **c** nitrogen and **d** iron contamination of samples welded under various conditions showing: low contamination and little change in hardness with increasing pulse power for low contamination conditions; high hardness which increases with pulse power along with significant O and N contamination for air contamination conditions; and moderate increase in hardness with pulse power along with significant Fe contamination for stage contamination conditions

seam in the form of a coloured oxide. Colouration is due to a thickening of the oxide layer, which changes how light interacts with the surface with the colour giving an indication of the oxide thickness. The colours observed on the surface of the seam for the samples welded under 'air' shielding conditions are summarised in Table 3. The colour of the weld seams corresponded well with the level of measured O contamination within the weld, indicating a progressively thicker oxide with increasing pulse power.

## Effect of bulk contaminants

The hardness of the fusion zone for the three alloys welded with a pulse power of 1.1 kW under low contamination conditions is given in Fig. 3. The hardness for the bulk substrate of each alloy after cold rolling and vacuum annealing at 750 °C for 2 h is also given for comparison. Alloy G1a underwent the least amount of hardening compared with the annealed bulk having an average hardness difference of 25 HV. Alloy G1b underwent more than twice this amount of hardening with an average difference

**Table 3** Colours predominant in weld seam for samples welded under poor shielding conditions

| Pulse power (kW) | Weld seam appearance |
|---|---|
| 1.10 | Silver/straw |
| 1.27 | Silver/straw/purple |
| 1.43 | Straw/purple |
| 1.60 | Straw/purple/blue |

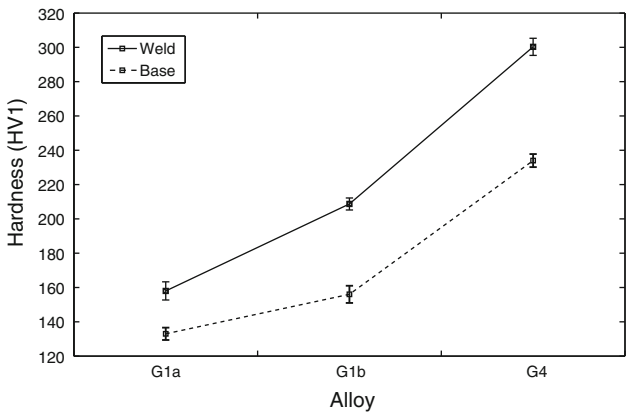


**Fig. 3** Weld fusion zone hardness for different CP Ti alloys for a pulse power of 1.1 kW compared to hardness of the annealed substrate showing significantly more hardening in alloys G1b and G4 than in alloy G1a

of about 53 HV, whilst G4 had an average difference of around 66 HV.

Whilst alloy G1a exhibited a columnar α structure as presented in Fig. 1, the other two alloys both formed acicular α in the fusion zone at a pulse power of 1.1 kW (Fig. 4). The acicular laths are much finer in the case of alloy G4 compared to G1b.

## Nature of the microstructural transformations

The columnar grain structures observed in the weld appear to be massive α due to both the irregular nature of the grain

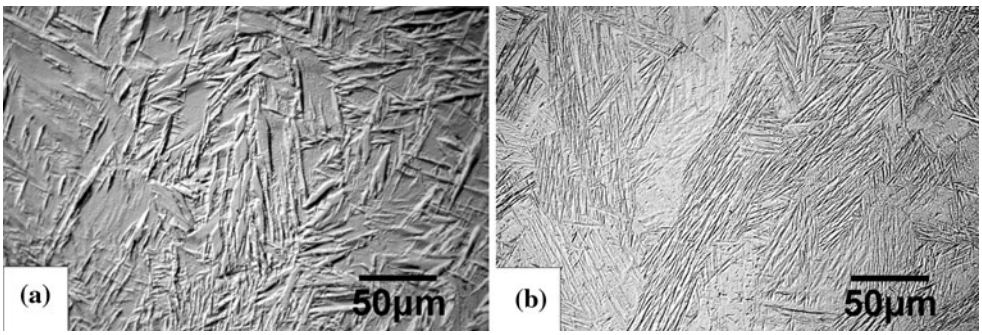


**Fig. 4** Fusion zone microstructures at a pulse power of 1.1 kW for **a** alloy G1b showing predominantly course acicular α and **b** alloy G4 showing predominantly fine acicular α

boundaries, as reported elsewhere [12] and also the structure of the thermally etched surface grains. Electron micrographs of the thermally etched surface reveal grain boundaries, which appear to cross other etched grain boundaries (Fig. 5a). This is evidence that a massive transformation allowed α grains to grow independently of the β grain boundaries. Observation of the weld surface for the acicular microstructure suggests that these were formed by a martensitic transformation, as large tent-shaped displacements can be observed on the surface (Fig. 5b). This structure is therefore likely to be α' martensite.

## Discussion

The results associated with the uptake of contaminants during welding suggest that O and N contamination from the air only begin to affect the hardness and microstructure of the weld when the contamination becomes appreciable. Whilst a silver weld seam was maintained, the structure and hardness of the weld was largely unaffected, despite oxygen contamination of up to around 350 ppm. However, it is interesting that whilst a high level of O and N contamination from the air caused a large increase in hardness, they did not modify the nature of the allotropic phase transformation as much as the Fe contamination from the stage. Even with the highest level of about 900 ppm O and 1000 ppm N contamination from the air there was still a significant portion of massive α present in the microstructure. Compare this to the situation with 1800 ppm Fe contamination from the stage, which completely suppressed the massive transformation at a pulse power of 1.43 kW. Despite the higher degree of structure modification most of the samples with Fe contamination from the stage still had a lower hardness than the samples with O and N contamination from the air. It appears then that O and N cause a significant amount of solid solution strengthening, whilst the hardening due to Fe appears to be mainly due to martensite formation.

The Fe uptake from the stage was also accompanied by an uptake of O and N which, whilst lower than the samples welded under 'air' contamination conditions, was higher than samples welded under low contamination conditions. As there is no additional contamination in samples welded in close proximity to the Fe stage at 1.1 kW where stage interaction did not occur, this additional O and N contamination is likely to be a result of the stage interaction. Whilst developing good shielding conditions it was observed that contamination in the weld pool was highly sensitive to turbulence in the shielding gas. It is believed

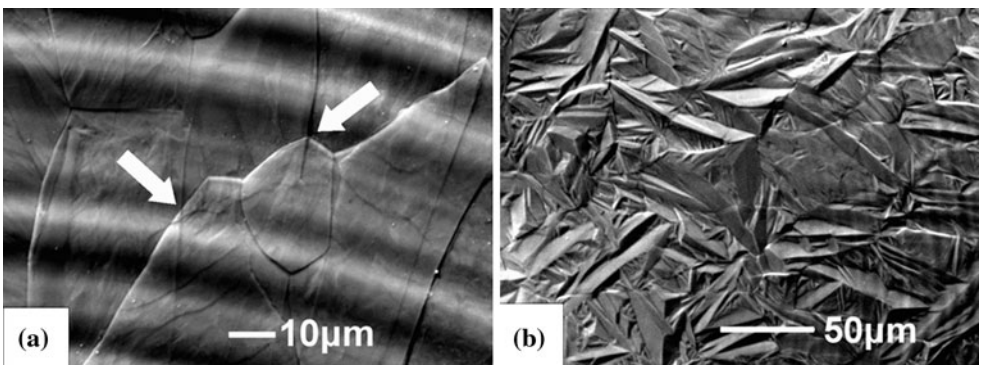


**Fig. 5** Surface observations of G1a alloy weld showing **a** crossing of thermally etched grain boundaries in low contamination weld performed at 1.1 kW and **b** tent like surface displacement in weld performed at 1.43 kW with contamination from stage

then that the turbulence caused by the stage interaction disrupted the stable shielding conditions on the underside of the weld (where most discolouration was observed) and caused more air contamination to be entrained in the weld pool.

It is also interesting to note that, despite having the same ASTM classification, alloys G1a and G1b had dramatically different responses to welding in respect to both microstructure and the degree of hardening. Whilst there existed a small difference in hardness between the annealed substrates, alloy G1b underwent more than twice the level of hardening in the weld seam and showed a martensitic rather than massive transformation. This demonstrates the inadequacy of relying on ASTM classification alone to compare the response of different titanium alloys. If we look at the composition of these two alloys we find that G1a has a higher O and N content than G1b, but the Fe concentration in G1b is higher. This adds further support to the assertion that Fe strongly promotes the formation of martensite, even more so than O and N, which researchers have tended to focus on in the literature.

Alloy G4 has a much higher level of O and Fe contamination in the bulk, which caused refinement of the laths and further hardening. Although the hardness of the annealed substrate and the level of contamination of alloy G4 were much higher than that of alloy G1b, there was not that much difference in the degree of weld hardening between them. In the case of bulk contaminants solid solution strengthening would not affect the degree of hardening as it affects both the bulk and the weld. The most important aspect in avoiding weld hardening then seems to be avoiding the martensitic transformation. Hence, Fe contamination in the bulk should be an important concern for avoiding weld hardening.

These results generally agree with other studies on pulsed laser welding of titanium. Two studies that observed columnar grains in the as-welded microstructure both reported lower Fe contamination than the alloy G1b used here. Fujioka et al. [11] used a base alloy with a composition of 930 ppm O, 30 ppm N, 480 ppm Fe, whilst Asahina et al. [4] reported a composition of 100 ppm O, 100 ppm N and 700 ppm Fe. Unfortunately not many more comparisons can be made to other literature on pulsed laser welding of CP titanium alloys, because the composition of the alloy is often not reported and, as demonstrated here, the ASTM grade alone is insufficient to characterise the material.

Chon and Park [13] performed a fundamental investigation into the effect of Fe on the continuous cooling $\alpha$–$\beta$ phase transformation behaviour in CP Ti. They found that an alloy with 800 ppm Fe exhibited a massive transformation up to a cooling rate of 700 °C/s, whilst the massive transformation was largely suppressed in an alloy with 2300 ppm Fe. As these values bound the Fe concentration of the G1b alloy, they are also consistent with the present conclusion that Fe had a significant effect on suppressing the massive transformation and favouring the formation of martensite. In contrast, Cormier and Claisse [14] found that oxygen concentrations up to 4000 ppm had little effect on the nature of the $\alpha$–$\beta$ phase transformation. Unfortunately no studies could be found on the effects of N.

As the massive transformation is a partitionless diffusional transformation then, in general, the addition of alloying elements will increase the energy barrier for the massive transformation and favour the diffusionless martensitic transformation. The reason that iron is far more effective at suppressing the massive phase compared with O and N is, however, more complicated especially given the fast diffusion rate of Fe in Ti which is faster than that of O [15]. It is believed that although the massive transformation is partitionless a small concentration spike (less than one interatomic spacing) can form behind the advancing $\alpha$ massive/$\beta$ interface due to short range diffusion [13, 16]. This concentration spike will limit the velocity of the interface and the larger the spike the slower the interface will proceed. As iron is a strong $\beta$ stabiliser it will be attracted to the $\beta$ side of the interface and segregate there. Thus, this segregation of iron will limit the massive transformation growth in a similar way that solutes attracted to a grain boundary limit the growth of the grain boundary [17]. Iron is added to titanium because it strongly segregates to the grain boundaries and retards the recrystallization kinetics. As the massive phase typically nucleates at grain boundaries, then iron can be expected to suppress the nucleation and growth of the massive transformation. As oxygen and nitrogen are interstitial and are $\alpha$ stabilizers, they do not tend to segregate to grain boundaries as strongly as iron, and so they do not have the same effect on the kinetics of the transformation.

## Conclusions

In light of the present results we conclude that:

- During pulsed laser welding with low levels of contamination the nature of the allotropic phase transformation is massive and increasing the level of contaminants acts to suppress this transformation and encourage the formation of martensite.
- Despite a focus on O and N in the literature, it appears that Fe is a stronger promoter of the martensitic phase during pulsed laser welding, due to its high level of segregation. O and N cause a significant amount of solid solution strengthening.
- Knowledge of the ASTM grade of titanium is not sufficient to predict the response to pulsed laser welding in CP alloys.

– The level of atmospheric contamination was not a concern, until evidence of significant contamination was observed through colouration of the surface oxide.

The individual effects of O and N are still largely unclear. Future research will focus more on decoupling the role of O and N and analysing the effects of bulk contaminants more accurately within the context of Ti–O, Ti–N and Ti–Fe binary alloys.

**Acknowledgements** The authors would like to acknowledge the support of the CAST Cooperative Research Centre. CAST was established and is supported by the Australian Government's Cooperative Research Centre Programme.

## References

1. Schneider R (2009) J Esthet Restor Dent 21:215
2. Waurzyniak P (2010) Manuf Eng 144:59
3. Anselm Wiskott HW, Doumas T, Scherrer SS, Belser UC (2001) J Mater Sci Mater M 12:719
4. Asahina T, Itoh Y (2005) J Jpn I Light Met 55:337
5. Richter K, Behr W, Reisgen U (2007) Materialwiss Werkst 38:51
6. Liu J, Watanabe I, Yoshida K, Atsuta M (2002) Dent Mater 18:143
7. Wang R, Welsch G (1995) J Prosthet Dent 74:521
8. Yamagishi T, Ito M, Fujimura Y (1993) J Prosthet Dent 70:264
9. Huang HH, Lin SC, Lee HK, Chen C (2005) J Mater Sci 40:789. doi:10.1007/s10853-005-6325-6
10. Li X, Xie J, Zhou Y (2005) J Mater Sci 40:3437. doi:10.1007/s10853-005-0447-8
11. Fujioka S, Kakimoto K, Inoue T, Okazaki J, Komasa Y (2003) Dent Mater J 22:581
12. Oh M, Lee JY, Park JK (2004) Metall Mater Trans A 35:3071
13. Chon SH, Park JK (2005) In: Proceedings of an international conference on solid-solid phase transformations in inorganic materials. Minerals, Metals and Materials Society, Phoenix, p 755
14. Cormier M, Claisse F (1974) J Less Common Met 34:181
15. Nakajima H, Koiwa M (1991) ISIJ International 31:757
16. Plichta M, Williams JC, Aaronson H (1977) Metall Trans A 8:1885
17. Hillert M, Sundman B (1976) Acta Mater 24:731